

Characteristics and Radiative Effects of Diamond Dust over the Western Arctic Ocean Region

JANET M. INTRIERI

NOAA/Environmental Technology Laboratory, Boulder, Colorado

MATTHEW D. SHUPE

Science and Technology Corporation, NOAA/Environmental Technology Laboratory, Boulder, Colorado

(Manuscript received 28 August 2003, in final form 19 February 2004)

ABSTRACT

Atmospheric observations from active remote sensors and surface observers, obtained in the western Arctic Ocean between November 1997 and May 1998, were analyzed to determine the physical characteristics and to assess the surface radiative contribution of diamond dust. The observations showed that diamond dust contributed only a negligible radiative effect to the sea ice surface. Surface radiative fluxes and radiative forcing values during diamond dust events were similar in magnitude when compared to observed clear-sky periods. Combined information from lidar, radar, and surface observers showed that diamond dust occurred ~13% of the time between November and mid-May over the Arctic Ocean and was not observed between mid-May and October. Diamond dust vertical depths, derived from lidar measurements, varied between 100 and 1000 m but were most often observed to be about 250 m.

Lidar and radar measurements were analyzed to assess if precipitation from boundary layer clouds was present during times when surface observers reported diamond dust. This analysis revealed that surface observers had incorrectly coded diamond dust events ~45% of the time. The miscoded events occurred almost exclusively under conditions with limited or no illumination (December–March). In 95% of the miscoded reports, lidar measurements revealed the presence of thin liquid water clouds precipitating ice crystals down to the surface.

1. Introduction and background

Unraveling the effects of clouds on the surface energy budget of the Arctic has seen recent advancement. These advances can be attributed to 1) an increased research emphasis precipitated by climate-warming concerns at high latitudes and 2) the resulting long-needed observational information gathered from newly acquired oceanic, ice, and atmospheric datasets. For example, year-long cloud measurements, collected over the Beaufort and Chukchi Seas during 1997/98, provided key information for compiling an annual cycle of Arctic cloudiness statistics (Intrieri et al. 2002b) and for quantifying an annual cycle of cloud radiative forcing over the Arctic surface (Intrieri et al. 2002a). This same Arctic cloud dataset has been analyzed by Shupe and Intrieri (2004) to assess which cloud types are radiatively important and which individual cloud properties most affect the surface longwave and shortwave radiation.

Cloudless ice crystal precipitation (ICP), more com-

monly termed “diamond dust,” has been hypothesized to have a significant effect on the radiative balance at the Arctic surface (e.g., Gotaas and Benson 1965; Curry et al. 1990, 1993; Wilson et al. 1993). As part of the Shupe and Intrieri cloud–radiation study, diamond dust was found to provide only a negligible surface radiative contribution. Since diamond dust information is sparse, we present additional remote sensing and surface observations to provide further details on the frequency of occurrence and physical, microphysical, and radiative properties of this polar phenomena.

Observations of diamond dust are scarce because of the difficulties encountered when making measurements in the harsh polar environment, and suspect because surface observations are notoriously difficult due to the poor visibility during the dark winter season when diamond dust is most prevalent (Hahn et al. 1995). Additionally, satellite observations are not especially useful in detecting or characterizing diamond dust since there is little thermal or visible contrast between it and the underlying snow- and ice-covered surface. Diamond dust is not explicitly included in classic cloud climatologies, so long-term statistics of its occurrence are not available. Even more rare are microphysical and radi-

Corresponding author address: Dr. Janet M. Intrieri, NOAA/Environmental Technology Laboratory, 325 Broadway, R/E/ET2, Boulder, CO 80305.

E-mail: janet.intrieri@noaa.gov

ative observations of ICP; those that do exist are highly sporadic, short in duration, and exhibit a wide range of values (e.g., Gotaas and Benson 1965; Witte 1968; Ohtake et al. 1982; Curry et al. 1990; Pinto et al. 2001).

Several modeling studies have explored the role of diamond dust on the Arctic surface radiation budget. Curry and Ebert (1992) concluded that the presence of tropospheric ICP has little direct effect on the net top-of-atmosphere (TOA) fluxes, but can have a substantial IR radiative impact at the surface since it occurs near the surface and at near-surface temperatures. They proposed the addition of ICP as a separate winter cloud category in order to derive internally consistent annual cycles of cloud, surface, and atmospheric properties. It has also been theorized that the presence of ICP may have a dominant effect on Arctic visibility. Meyer et al. (1991) demonstrated through modeled visual ranges that aerosol alone did not account for the low observed Arctic visibilities. When ice was included along with the aerosol, modeled visibilities were reproduced in the ranges that have been observed. In a single case of ICP observed in autumn, Pinto (1998, 2001) calculated a much smaller radiative signal at the surface of about 5 W m^{-2} . More recently, Girard and Blanchet (2001) have simulated smaller-scale physical processes in the Arctic using a model focusing primarily on aerosol–cloud interactions. In their model study, a radiative contribution as high as 60 W m^{-2} was reported for, what they termed, a “mixed phase” diamond dust event in which a thin liquid cloud layer was present at the top of the surface-based inversion and above the diamond dust.

Unfortunately, previous studies, statistics, model results, and working hypotheses have had to rely on limited observations of diamond dust. Thus, large uncertainties exist regarding its frequency of occurrence, microphysical characteristics, and radiative impact. Obtaining longer-term, integrated, and comprehensive measurements on diamond dust and on Arctic clouds in general, in order to improve our understanding and modeling of the Arctic radiation budget, was one of the observational goals of the Surface Heat Budget of the Arctic Ocean (SHEBA) program (Uttal et al. 2002). SHEBA was an international, interdisciplinary, and multiagency program led by the National Science Foundation. It was designed to investigate and characterize Arctic oceanic, atmospheric, and sea ice properties over an entire annual cycle. During the field phase of SHEBA, a variety of active and passive instruments were deployed, for a 1-yr period starting in October of 1997, from an icebreaker that drifted with the ice pack on a 2800-km path from 75°N , 143°W to 79°N , 166°W . All observations presented in this paper were gathered as part of the SHEBA program.

2. Diamond dust observations

a. Instrumentation and analysis

Observations of diamond dust and cloud occurrence, heights, and phase were obtained during SHEBA by a

combination of measurements from ground-based lidar and radar. These vertically pointing, range-resolved active remote sensing instruments were developed at the National Oceanic and Atmospheric Administration/Environmental Technology Laboratory (NOAA/ETL) specifically for operation in the harsh Arctic environment. Broadband radiometers at the surface provided infrared and solar fluxes. Details and specifications on the lidar, radar, and radiometer instruments can be found in Intrieri et al. (2002b) and Persson et al. (2002).

Ground-based lidar and radar are not optimal for detecting diamond dust because the lowest resolved range gates are nominally sampled at 90 and 105 m, respectively. Typically, the radar was not sensitive enough to have consistent returns from diamond dust and, therefore, was used only to identify clear-sky versus cloudy conditions. Depolarization ratio measurements from lidar were used to discriminate between water and ice phases and to determine ICP layer depths when they exceeded the minimum range of 90 m.

SHEBA surface observers logged entries of weather conditions every 6 h with diamond dust, ice crystals, or ice fog recorded as a specific weather code if observed. In order to obtain microphysical information, a handheld ice crystal replicator was used to capture diamond dust samples on three occasions. Formvar-coated, 35-mm clear film, dissolved by chloroform that was administered by hand, was spooled across an open-air area onto which the crystals fell and were captured. The films were then viewed under a microscope and digital pictures were obtained.

b. Diamond dust frequency of occurrence

Generally defined, diamond dust is crystalline condensation that can occur throughout the cold half of the year (October–April) within the Arctic stable boundary layer when air temperatures are sufficiently low. Diamond dust is composed of suspended ice particles in an otherwise cloudless environment, often appearing as an ice fog. In many of our lidar and radar measurements, boundary layer mixed-phase clouds were observed precipitating ice crystals down to the surface, but we do not consider this to be diamond dust.

Lidar, radar, longwave (LW) and shortwave (SW) radiometer, and surface observer datasets acquired between 1 November 1997 and 2 October 1998 were examined to determine the frequency of diamond dust occurrence. During this analysis period, surface observer log entries reported diamond dust or ice crystals on 188 occasions. A log entry was deemed incorrect if either the lidar or radar revealed a boundary layer cloud with precipitation. If no cloud was observed during a logged event, then the surface observation was assumed to be correct. Out of the 188 cataloged events, 88 events (~47%) were incorrectly reported by the observers, with the lidar and radar revealing the presence of clouds and precipitation, and 100 events (~53%) were cor-

TABLE 1. Monthly statistics of diamond dust events and reporting accuracy.

Month	No. of diamond dust events reported by surface observers	No. of events (%) when the remote sensors saw precipitating clouds	No. of events (%) when clouds containing LW were observed during diamond dust reports
Nov 1997	4	3 (75%)	3 (75%)
Dec 1997	48	17 (35%)	17 (100%)
Jan 1998	48	25 (52%)	25 (100%)
Feb 1998	50	23 (46%)	23 (100%)
Mar 1998	22	14 (62%)	13 (93%)
Apr 1998	15	6 (40%)	3 (50%)
May 1998	1	0 (0%)	NA
Jun–Sep	0	NA	NA
Nov–Sep total	188	88 (47%)	84 (95%)
(1–9 Oct 1998)	(5)	Not included in study since neither the lidar nor radar were operating	

rectly assessed as diamond dust. See Table 1 for the monthly breakdown of surface observer reports and accuracy statistics.

Analysis of the combined active remote sensing and surface observer reports suggests that diamond dust occurred $\sim 13\%$ of the time between 1 November 1997 and 10 May 1998 at the SHEBA ship located in the south-central Arctic Ocean region [(100 correctly logged ICP events)/(194 days \times 4 reports per day of possible events)]. Note that this percentage may be underestimated due to ICP events that were missed by the surface observers. Diamond dust was not observed between 11 May and 2 October (2 October marking the end of the lidar and radar measurements). Because ICP climatologies are rare, comparisons with previous findings in the same region are practically impossible. One study, however, using climate data spanning many years from different Canadian Arctic stations (Maxwell 1982), showed a greater frequency of ICP occurrence than was observed in the SHEBA region, with maximum values varying between 20% and 50% during winter, and the same result of zero occurrence during summer.

The majority of miscoded SHEBA diamond dust events occurred under conditions of little or no direct sunlight (December–March) and during times when the lidar observed thin liquid water clouds precipitating ice crystals. Lidar depolarization ratio measurements confirmed the presence of liquid water clouds in practically all of the incorrectly coded events ($\sim 95\%$). These thin water clouds, most often residing between 250 and 1000 m, were observed an average of 50% of the time when clouds were observed during the cold and dark SHEBA months (Intrieri et al. 2002b). These mixed-phase clouds were also found to have profound and immediate effects on the winter longwave surface radiation, especially in comparison to that of clear skies, high ice clouds, and diamond dust (Shupe and Intrieri 2004).

c. Diamond dust physical characteristics

The lidar's depolarization ratio information revealed ice condensate whenever the diamond dust extended above the minimum range. These events were analyzed to infer some general physical characteristics about the diamond dust events. ICP vertical depths (remembering to note that the lidar's minimum range precluded observing events less than 90 m in depth) were most commonly observed to be ~ 250 m, with maximum depths up to 1 km being observed on two occasions. Although the lidar scanned from horizon to horizon in the spring and summer, it only obtained vertically pointing measurements during the winter. It therefore could not provide information on the horizontal extent of the ICP. Temporally, ICP events were highly variable, lasting anywhere from several hours up to 5 days.

In order to obtain microphysical information, diamond dust ice crystal samples were obtained using a handheld replicator from the top of the icebreaker (~ 20 m AGL) on three separate occasions (with surface temperatures at -40° , -39° , and -24°C), each over a period of approximately 30–45 min. Unfortunately, the sampling periods are not sufficient to obtain statistical or quantitative data, but are presented nonetheless since microphysical measurements of diamond dust are rare.

The replicator film revealed myriad ice crystal habits measuring between approximately 50 and 250 μm (Fig. 1). The most common shapes included shizus (very thin needles), hexagonal plates, columns, and scrolls (open and hollow hexagonal plates), with occasional trigonals, which form only in very low temperatures (A. Heymsfield 2003, personal communication). A quite apparent difference in crystal habit was observed between the samples obtained during the two days at $\sim -41^\circ\text{C}$ and the warmer day at $\sim -24^\circ\text{C}$. The colder days were characterized predominantly by dense concentrations of shizus of varying lengths, whereas the warmer day yielded columns, plates, and larger individual crystal shapes.

d. Diamond dust radiative impact

Since wintertime surface IR fluxes have been observed to be 10–40 W m^{-2} greater than modeled clear-sky values (e.g., Overland and Guest 1991), it has been inferred that ICP may be responsible for the additional downwelling flux (Curry and Ebert 1992). The Curry and Ebert (1992) model results represent an internally consistent set of radiation parameters; however, they note that the solutions are not necessarily unique. This is because varying cloud parameters in the model can produce other, equally consistent, solutions. Given the extremely low winter temperatures and the lack of active, remote profiling sensors such as lidar and radar, their ICP inference is reasonable. In another more recent study, Girard and Blanchet (2001), using a model developed primarily on the aerosol–cloud interactions that

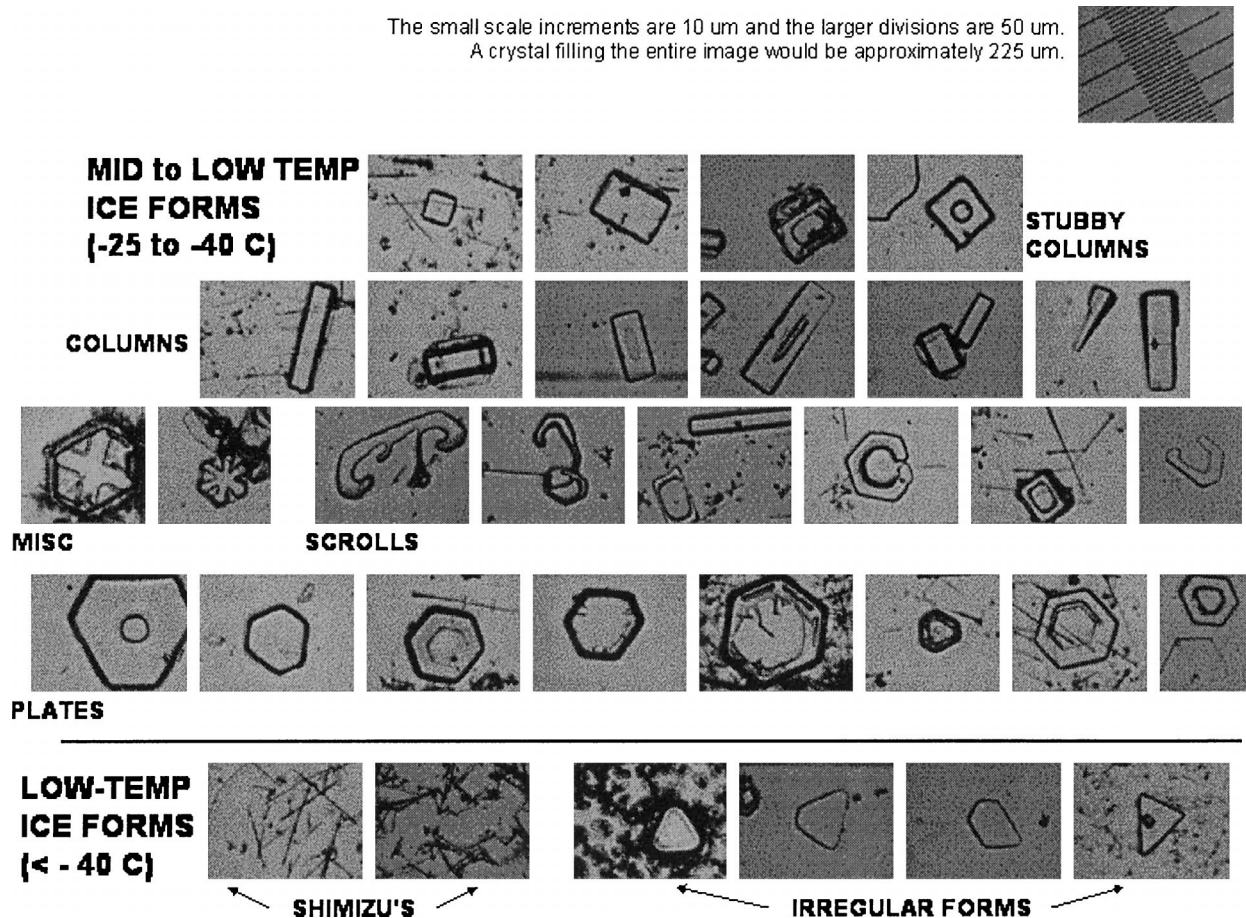


FIG. 1. Ice crystal montage compiled from images obtained during SHEBA with a handheld replicator. A single crystal filling an entire box is approximately 225 μm in diameter.

form ice crystals in stable air, reported modeled mixed-phase diamond dust (ice crystals present under a liquid water cloud near the inversion layer), contributing up to 60 W m^{-2} to the downward IR radiation flux at the surface in winter.

At SHEBA, we commonly observed enhancements in the wintertime LW surface flux of between 20 and 40 W m^{-2} ; however, they were exclusively attributed to shallow liquid water clouds that reside at or near the ever-present inversion layer and precipitate ice crystals. Conversely, surface LW fluxes were not observed to be significantly affected by the presence of ICP. Thus, we contend that the marked wintertime surface flux increases are not due to the ICP, but to the thin liquid water (mixed phase) clouds observed by lidar to occur frequently during winter and form at temperatures as low as $\sim -35^{\circ}\text{C}$ (Intrieri et al. 2002b). These commonly observed water clouds precipitating ice crystals are very similar to and confirm the Girard and Blanchet (2001) model simulations in terms of the radiative forcing from their mixed-phase diamond dust.

In order to quantitatively distinguish the surface radiative effects of clouds and ICP, two diamond dust case

study events were analyzed. These events were identified from surface observations and confirmed by lidar and radar measurements. The first case spanned the period from 27 December 1997 through 1 January 1998 and the second from 15 through 20 January 1998. Data from two radiometric instruments were examined to assess the surface radiative effect from the ICP—one obtained by a broadband hemispheric IR radiometer (Persson et al. 2002) and the other obtained by an Atmospheric Emitted Radiance Interferometer (AERI; Smith et al. 1999).

No significant surface radiative effects were detected during diamond dust events from either of the aforementioned radiometric observations. The broadband radiometer registered no appreciable differences in the upwelling or downwelling surface LW fluxes between clear-sky and ICP conditions. Further, using the more detailed radiative information from the AERI, brightness temperatures at IR wavelengths also revealed little difference between clear-sky and ICP events. In contrast, the occurrence of water clouds displayed strong identifiable signatures by both instruments.

These results are illustrated by the three case study

days presented in Fig. 2 depicting (a) lidar returned power, (b) lidar depolarization ratio, (c) broadband radiometer fluxes, and (d) AERI-derived IR brightness temperatures during periods of intermittent clear sky, diamond dust, and water-containing mixed-phase clouds. The “boxes” highlight times (0000–0200 UTC on 15 January and 0400–2000 UTC on 20 January) when clouds containing liquid water were detected by the lidar (characterized by greater returned power signatures and lower depolarization ratio values). Diamond dust was detected by the lidar (characterized by low returned power and high depolarization ratios) at the end of 15 January and most of the day on 17 January. (Note: the loss of lidar detector sensitivity on 15 January is reflected by the white areas for most of that day.) The solid square symbols in Fig. 2c on 15 January, between 0000 and 0200 UTC, correspond to flux values used from an adjacent radiometer set during a time period when the ETL broadband radiometer was not operational. The asterisks in Fig. 2d indicate times when the surface observers recorded the occurrence of diamond dust.

In both of the water cloud cases, broadband radiometer flux measurements displayed significant increases of up to 35 W m^{-2} and IR brightness temperature increases of between 10° and 30°C . By contrast, the clear-sky (e.g., 0000–0300 UTC on 17 January) and diamond dust events (in this case, $\sim 200 \text{ m}$ thick on 15 and 17 January) displayed negligible flux and brightness temperature signatures. From the analysis of sounding and flux tower data obtained during the case study, the trends in the broadband IR flux measurements in Fig. 2c corresponded to upper-level atmospheric temperature fluctuations from the baseline values (P. O. G. Persson 2003, personal communication). As illustrated by the three case study days, we generally found that, throughout the winter season, clear skies and diamond dust had similar radiative characteristics at the surface.

Accordingly, because no appreciable changes in the surface IR flux due to ICP were observed, surface radiative forcing estimates (the difference between observed surface fluxes when ICP was present and fluxes under modeled clear skies; see Intrieri et al. 2002a for details) only ranged between 0 and 6 W m^{-2} , which is within the estimated error range of the radiometer measurements and model uncertainties. In contrast, wintertime surface *cloud* radiative forcing (the difference between observed surface fluxes when clouds are present and fluxes under modeled clear skies) ranged between 15 and 30 W m^{-2} for ice clouds and 20 and 70 W m^{-2} for clouds containing liquid water (Shupe and Intrieri 2004).

3. Summary and discussion

Atmospheric and cloud observations obtained at SHEBA between November 1997 and May 1998 from lidar, radar, radiometers, and surface observers were analyzed to better understand the characteristics and ra-

diative impact of diamond dust. The SHEBA observations show the following:

- Surface observers incorrectly coded diamond dust events $\sim 45\%$ of the time. The miscoded events were determined by lidar and radar measurements to contain precipitating boundary layer clouds and occurred almost exclusively under conditions with limited or no illumination (December–March).
- In 95% of the miscoded diamond dust reports, lidar measurements revealed the presence of thin liquid water clouds that were precipitating ice crystals down to the surface.
- Diamond dust occurred $\sim 13\%$ of the time between November and mid-May at the SHEBA ship with vertical depths most commonly observed to be $\sim 250 \text{ m}$. Diamond dust was not observed to occur between mid-May and October.
- Replicator films obtained on three separate occasions revealed that the diamond dust was composed predominantly of very thin needles or shimizus when observed at $\sim -41^\circ\text{C}$ and predominantly of columns and hexagonal plates, ranging between 50 and $250 \mu\text{m}$, on a day when temperatures were recorded at $\sim -25^\circ\text{C}$.
- Diamond dust did not have a significant radiative effect at the SHEBA ship. Surface radiative fluxes were similar in magnitude to those observed during clear-sky events and radiative forcing values were on the order of the measurement and modeling uncertainties.

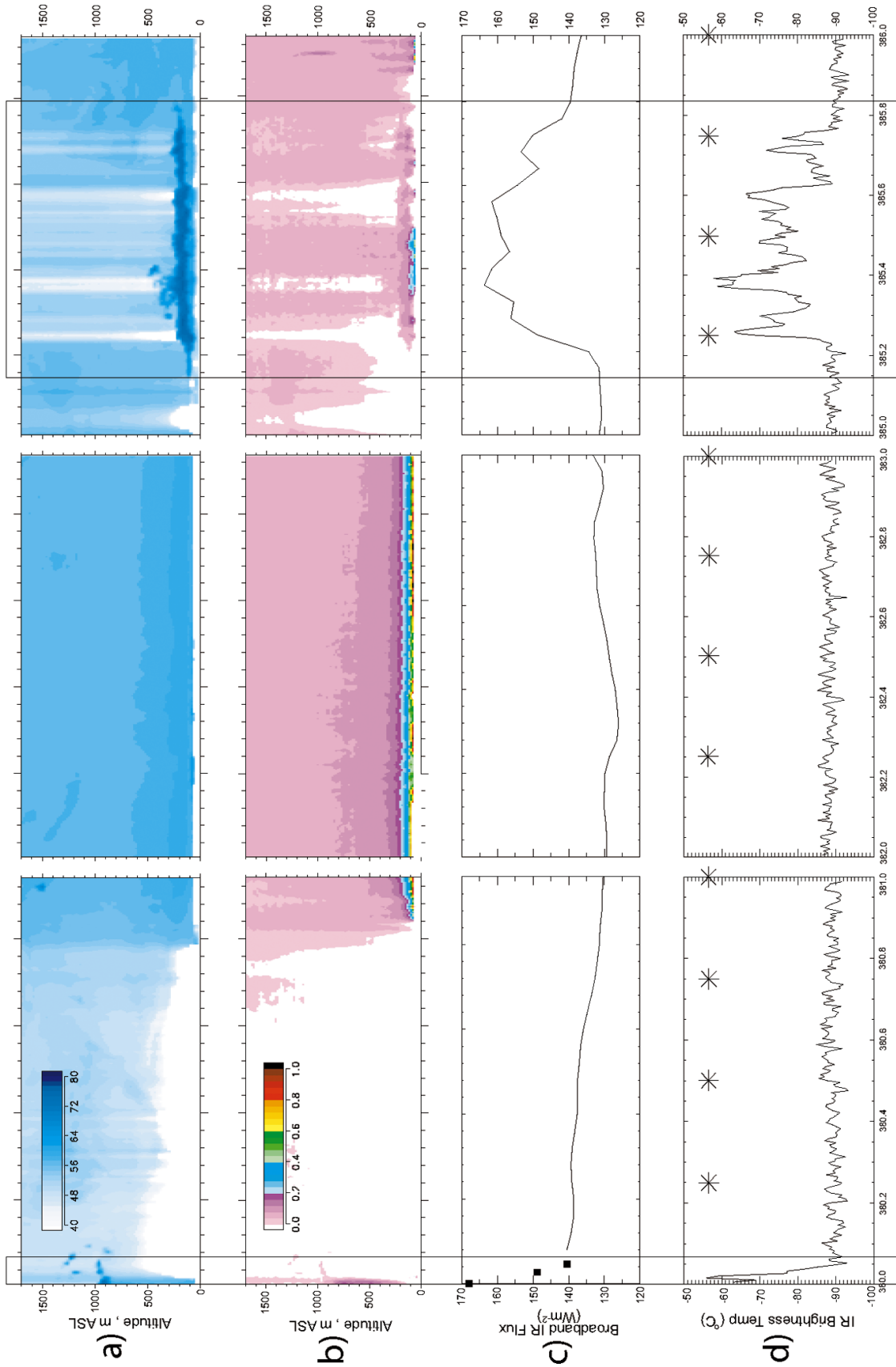
The observations in this paper represent one set of data for one year. However, in comparison to studies conducted in previous years, we surmise that diamond dust has had an inflated radiative role because wintertime liquid clouds have been historically underpredicted in climatologies and accordingly misparameterized in Arctic models. For example, in order to model the amount of observed LW flux from Arctic radiometer data, Curry et al. (1993) produced reasonable quantities by adding a persistent and thick layer of ICP into the modeled winter cloud types. Observations of water cloud occurrence during the Arctic winter had, as of the time of the Curry et al. study, not been commonly observed or reported. SHEBA observations show that the addition of a realistic number of thin water clouds as opposed to persistent ICP could also produce a correct radiative result. We suggest that Arctic cloud annual cycles or climatologies be modified to include a winter season low-level liquid water cloud frequency of occurrence and height category such as those based on lidar observations reported in Intrieri et al. (2002b). In this dataset, the lidar detected liquid water in $\sim 50\%$ of the clouds observed between December and March and at temperatures colder than typically predicted by models.

These observations suggest the need to modify parameterizations linking cloud phase and temperature. In addition to the water cloud occurrence and height sta-

20 January 1998

17 January 1998

15 January 1998



Time (Decimal Julian Day)

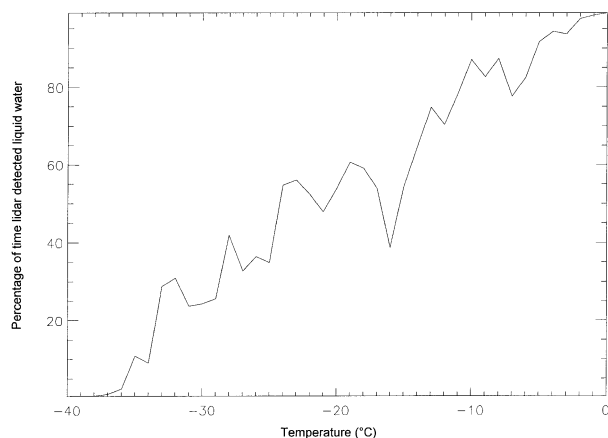


FIG. 3. Percentage of time the lidar determined the presence of liquid water in cloud vs the radiosonde interpolated cloud temperatures ($^{\circ}\text{C}$).

tistics, information relating cloud temperature and phase at SHEBA was obtained by interpolating radiosonde temperatures to the lidar cloud heights. Figure 3 illustrates the percentage of time that the lidar detected the presence of liquid water in clouds versus the cloud temperature over the annual cycle. Note that at temperatures less than -36°C , the lidar detected zero occurrences of liquid and at around 0°C the lidar detected 100% liquid occurrence. [A monthly breakdown of phase and temperature is illustrated in Fig. 11 of Intrieri et al. (2002b).]

Capturing the correct cloud phase is critical in order to model the surface radiation more realistically in the Arctic. The European Centre for Medium-Range Forecasts (ECMWF) model results were compared to SHEBA observations, revealing that the current phase parameterizations used in this model do not create enough liquid water clouds in the Arctic and thus underestimate the surface radiation warming (C. S. Bretherton 2003, personal communication). The comparison revealed that the overall cloud height determined by the ECMWF model compared reasonably well to observations; however, the model clouds had a much greater ratio of cloud ice to water than was observed by the lidar, which led to biases of up to 50 W m^{-2} in the downwelling surface LW and SW radiation.

We note again that the SHEBA dataset represents a single year of observations, with diamond dust events that did not occur as frequently, nor were as optically thick or physically deep, as has been observed in other years and in other locations around the Arctic. Whether the SHEBA region displayed greater or lesser occurrences of diamond dust than “typical” years remains to

be determined. Discrepancies between the SHEBA year and previous years with greater percentages of occurrence could stem from warmer-than-average springtime temperatures, anticyclonic versus cyclonic conditions, which are less favorable for diamond dust formation, or changing aerosol characteristics between previous decades and the present. Additionally, we emphasize that ICP may have a greater effect over land-based polar regions such as Canada, Greenland, or Antarctica, where it can be more frequent and persistent and have a greater impact on precipitation (Bromwich 1988), air chemistry, and ozone depletion (e.g., Barrie 1985), as well as aerosol and pollution issues and scavenging (Hoff 1988).

Acknowledgments. The authors thank Andy Heymsfield at the National Center for Atmospheric Research (NCAR) for information on ice crystal habits and for use of the replicator while at SHEBA and Alan Hills, also at NCAR, for the use of the microscope and imaging analysis tools to obtain the ice crystal images. Thanks to James Pinto (NCAR) for helpful suggestions on the manuscript. This research was supported by the National Science Foundation SHEBA Agreement OPP-9701730, the National Aeronautics and Space Administration FIRE-ACE Contract L64205D, and the Biological and Environmental Research Program, U.S. Department of Energy, Interagency Agreement DE-AI03-02ER63325. The AERI data were obtained from the U.S. DOE Atmospheric Radiation Measurement Program. Special thanks to the SHEBA project office at the University of Washington for providing the surface ship report data, the crew of the Canadian Coast Guard ship, *Des Grosseilliers*, and the entire ETL SHEBA team.

REFERENCES

- Barrie, L. A., 1985: Atmospheric particles: Their physical and chemical characteristics and deposition processes relevant to the chemical composition of glaciers. *Ann. Glaciol.*, **7**, 100–108.
- Bromwich, D. A., 1988: Snowfall in high southern latitudes. *Rev. Geophys.*, **26**, 149–168.
- Curry, J. A., and E. E. Ebert, 1992: Annual cycle of radiation fluxes over the Arctic Ocean: Sensitivity to cloud optical properties. *J. Climate*, **5**, 1267–1280.
- , F. G. Meyer, L. F. Radke, C. A. Brock, and E. E. Ebert, 1990: Occurrence and characteristics of lower tropospheric ice crystals in the Arctic. *Int. J. Climatol.*, **10**, 749–764.
- , J. L. Schramm, and E. E. Ebert, 1993: Impact of clouds on the surface radiation balance of the Arctic Ocean. *Meteor. Atmos. Phys.*, **51**, 197–217.
- Girard, E., and J.-P. Blanchet, 2001: Simulation of Arctic diamond dust, ice fog, and thin stratus using an explicit aerosol–cloud–radiation model. *J. Atmos. Sci.*, **58**, 1199–1221.

←

FIG. 2. Three case study days obtained during SHEBA on (left) 15 Jan, (center) 17 Jan, and (right) 20 Jan. For each day (a) lidar returned power (dB), (b) lidar depolarization ratio (unitless), (c) broadband radiometer longwave flux (W m^{-2}), and (d) AERI-derived brightness temperatures ($^{\circ}\text{C}$) are pictured. Boxes indicate times when water cloud was detected by the lidar. All times are in UTC and heights are in km AGL.

- Gotaas, Y., and C. S. Benson, 1965: The effect of suspended ice crystals on radiative cooling. *J. Appl. Meteor.*, **4**, 446–453.
- Hahn, C. J., S. G. Warren, and J. London, 1995: The effects of moonlight on observation of cloud cover at night and application to cloud climatology. *J. Climate*, **8**, 1429–1446.
- Hoff, R. M., 1988: Vertical structure of Arctic haze observed by lidar. *J. Appl. Meteor.*, **27**, 125–139.
- Intrieri, J. M., C. W. Fairall, M. D. Shupe, P. O. G. Persson, E. L. Andreas, P. S. Guest, and R. M. Moritz, 2002a: An annual cycle of Arctic surface cloud forcing at SHEBA. *J. Geophys. Res.*, **107**, 8039, doi:10.1029/2000JC000439.
- , M. D. Shupe, T. Uttal, and B. J. McCarty, 2002b: An annual cycle of Arctic cloud characteristics observed by radar and lidar at SHEBA. *J. Geophys. Res.*, **107**, 8030, doi:10.1029/2000JC000423.
- Maxwell, J. B., 1982: *The Climate of the Canadian Arctic Islands and Adjacent Waters*. Vol. 2, *Climatological Studies*, Ministry of Supply and Services, Canada, 589 pp.
- Meyer, F. G., J. A. Curry, C. A. Brock, and L. F. Radke, 1991: Springtime visibility in the Arctic. *J. Appl. Meteor.*, **30**, 342–357.
- Ohtake, T., K. O. L. F. Jayaweera, and K.-I. Sakurai, 1982: Observation of ice crystal formation in lower Arctic atmosphere. *J. Atmos. Sci.*, **39**, 2898–2904.
- Overland, J. E., and P. S. Guest, 1991: The Arctic snow and air temperature budget over the sea ice during winter. *J. Geophys. Res.*, **96**, 4651–4662.
- Persson, P. O. G., C. W. Fairall, E. L. Andreas, P. Guest, and D. Perovich, 2002: Measurements near the Atmospheric Surface Flux Group tower at SHEBA: Near-surface conditions and surface energy budget. *J. Geophys. Res.*, **107**, 8045, doi:10.1029/2000JC000705.
- Pinto, J. O., 1998: Autumnal mixed-phase cloudy boundary layers in the Arctic. *J. Atmos. Sci.*, **55**, 2016–2038.
- , J. A. Curry, and J. M. Intrieri, 2001: Cloud–aerosol interactions during autumn over the Beaufort Sea. *J. Geophys. Res.*, **106**, 15 077–15 097.
- Shupe, M. D., and J. M. Intrieri, 2004: Cloud radiative forcing of the Arctic surface: The influences of cloud properties, surface albedo, and solar zenith angle. *J. Climate*, **17**, 616–628.
- Smith, W. L., W. F. Feltz, R. O. Knuteson, H. R. Revercomb, H. B. Howell, and H. H. Woolf, 1999: The retrieval of planetary boundary layer structure using ground-based infrared spectral radiance measurements. *J. Atmos. Oceanic Technol.*, **16**, 323–333.
- Uttal, T., and Coauthors, 2002: The Surface Heat Budget of the Arctic Ocean. *Bull. Amer. Meteor. Soc.*, **83**, 255–275.
- Wilson, L. D., J. A. Curry, T. P. Curry, and T. P. Ackerman, 1993: Satellite retrieval of lower-tropospheric ice crystal clouds in the polar regions. *J. Climate*, **6**, 1467–1472.
- Witte, H. J., 1968: Airborne observations of cloud particles and infrared flux density (8–14 microns) in the Arctic. M.S. thesis, Dept. of Atmospheric Sciences, University of Washington, 102 pp.